Journal of Alloys and Compounds 509 (2011) 3183–3189

Contents lists available at ScienceDirect

Journal of Alloys and Compounds

journal homepage: www.elsevier.com/locate/jallcom

Physical and optical studies in mixed alkali borate glasses with three types of alkali ions

M.A. Samee [a], A.M. Awasthi [b], T. Shripathi [b], Shashidhar Bale [a], Ch. Srinivasu [a], Syed Rahman [a,*]

[a] *Department of Physics, Osmania University, Hyderabad 500 007, India*
[b] *Consortium for Scientific Research, Khandwa road, Indore 452 017, India*

ARTICLE INFO

Article history:
Received 20 February 2010
Received in revised form 4 December 2010
Accepted 7 December 2010
Available online 15 December 2010

Keywords:
Mixed alkali effect
Density
Glass transition temperature
Optical absorption
Band gap energy
Glasses

ABSTRACT

So far only a handful of publications have been concerned with the study of the mixed alkali effect in borate glasses containing three types of alkali ions. In the present work, the mixed alkali effect (MAE) has been investigated in the glass system $(40-x)Li_2O-xNa_2O-10K_2O-50B_2O_3$. ($0 \leq x \leq 40$ mol%) through density and modulated DSC studies. The density and glass transition temperature of the present glasses varies non-linearly exhibiting mixed alkali effect. The glass stability is observed to be less which may be important for the present glasses as promising material for non-optical applications. We report, for the first time, the mixed alkali effect in the present glasses through optical properties. From the absorption edge studies, the values of indirect optical band gap (E_{opt}), direct optical band gap and Urbach energy (ΔE) have been evaluated. The values of E_{opt} and ΔE show non-linear behavior with compositional parameter showing the mixed alkali effect. The average electronic polarizability of oxide ions $\alpha_{O^{2-}}$, optical basicity Λ, and Yamashita–Kurosawa's interaction parameter A have been examined to check the correlations among them and bonding character. Based on good correlation among electronic polarizability of oxide ions, optical basicity and interaction parameter, the present $Li_2O-Na_2O-K_2O-B_2O_3$ glasses are classified as normal ionic (basic) oxides.

1. Introduction

A glass exhibits non-linear variation in its properties that include density, viscosity, glass transition temperature and conductivity when one alkali component in a multi component glass is systematically replaced by another species [1–3]. Besides the glasses containing only alkali ions, this non-linear behavior is exhibited by certain mixed alkali–alkaline earth oxide glasses also [4]. This phenomenon is referred to as 'mixed alkali effect' and is useful in manufacturing low loss electrical glass [1]. To study the mixed alkali phenomenon, borate glasses proved to be promising hosts to investigate the influence of chemical environment, structural diversity of ligand groups and spectroscopic properties of the materials [5]. In spite of numerous investigations, there appears to be no universally accepted mechanism for various mixed alkali effects.

Recently, Belostotsky [6] reported a new defect model for the mixed alkali effect. The essential physical concept involved is that simultaneous migration of two unlike alkali ions in mixed ionic glass accompanied by an expansion or contraction of the guest occupied sites with distortion of the surrounding glass matrix [7].

Far infrared spectroscopy has been employed to probe the effect of alkali mixing on the interactions between alkali ions and local sites in mixed alkali glasses [8,9]. Maass et al. [10] developed the dynamic structure model to explain the mixed alkali effect. The essential feature of this model is that the ionic mobility is drastically reduced because conduction pathways are effectively blocked due to the mismatch of the unlike cation sites. Many features of the MAE discussed by Ingram et al. [11] can be understood in terms of the glass network-mediated coupling between motions of dissimilar alkali ions and this indicates the maximum in the activation volume for ion transport.

Many investigations have been reported on mixed alkali effect in phosphate, borate, tellurite, bismuthate and silicate glasses which contain alkali and/or alkaline earth oxides [12–19]. More recently, Venkateswarlu et al. [20] presents the optical absorption and emission properties of Pr^{3+} and Nd^{3+} doped mixed alkali chloroborate glasses. The variation of Judd–Ofelt parameters, total radiative transition probabilities, radiative lifetimes and emission cross-sections with alkali contents in the glass matrix were discussed. The mixed alkali effect in the population of spin levels in $Li_2O-Cs_2O-B_2O_3$ glasses doped with Cr^{3+} ions was reported [21]

---

* Corresponding author. Tel.: +91 40 27095200; fax: +91 40 27090020.
E-mail address: syedrahman848@yahoo.co.in (S. Rahman).

0925-8388/$ – see front matter © 2010 Elsevier B.V. All rights reserved.
doi:10.1016/j.jallcom.2010.12.039

by studying electron paramagnetic resonance, optical absorption and luminescence techniques.

In our previous papers [22–24] we reported the mixed alkali effect in density, glass transition temperature, optical absorption and electron paramagnetic resonance of the mixed alkali boroarsenate and borobismuthate glasses.

Most technical glasses containing a variety of different cations, but almost all studies on mixed alkali effects are focused on glasses with only two kinds of ions. Therefore, it is very important to study ion dynamics of glasses with three or more types of alkali ions. To the best of our knowledge dynamic conductivity spectra of few Li–Na–K-containing borate glasses have been reported [25–27]. More recently, Kim et al. [28] reported the results of the composition dependence of the ionic conductivity in borate glasses with three types of mixed alkali cations.

In the present study, we investigate the mixed alkali effect in $(40-x)Li_2O–xNa_2O–10K_2O–50B_2O_3$ $(0 \leq x \leq 40$ mol%) glasses by measuring density and glass transition temperature as a function of compositional parameter R_{Na} which is defined as $R_{Na} = Na_2O$ (mol%)/$(Na_2O + Li_2O)$(mol%) which takes the values 0, 0.25, 0.5, 0.75 and 1. Further, optical studies have also been performed on glass samples.

2. Experimental

2.1. Glass preparation

In the present study, the glass samples of composition $(40-x)Li_2O–xNa_2O–10K_2O–50B_2O_3$ were prepared by melt quench technique. Starting materials for the glass preparation were Li_2CO_3, Na_2CO_3, K_2CO_3, (all GR grade, Merck) and boric acid (GR grade). Glasses were prepared by mixing the required proportions of the reagents in an electrical furnace using silica crucible. The furnace temperature was varied from 950 to 1050 °C depending on the glass composition. The liquids were agitated for 1 h to ensure homogeneous mixture. In this technique, the clear liquid (free of bubbles) is quickly cast in a stainless steel mould kept at 200 °C and pressed with another steel disc maintained at the same temperature. All the glass samples were then annealed at 200 °C for a duration of about 12 h. For samples taken from different regions of the bulk specimen, the absence of any Bragg peaks in the X-ray diffraction pattern confirmed that they are amorphous.

2.2. Density

Density (ρ) measurements were carried out at room temperature using Archimedes method with Xylene (density = 0.86 g/cc) as an immersion liquid. The uncertainty in density measurement is ± 0.001. Molar volume (V_m) = M/ρ, where M is the molecular weight of the glass expressed as the mole fractions of the oxides multiplied by their molecular weights. From the density data oxygen packing density were carried out using the formula:

Oxygen packing density = $(\rho/M)^*$ number of oxygen atoms per formula unit.

2.3. Glass transition temperature

The thermal behavior of the glass samples was investigated using a modulated differential scanning calorimeter (TA Instruments model 2910). Samples in the form of powder weighing about 15 mg were sealed in aluminum pans and scanned with a heating rate of 10 °C/min. During all runs the sample chamber was purged with dry nitrogen. The uncertainty in glass transition temperature is ± 1 °C.

2.4. Optical absorption

The room temperature optical absorption spectra for all the polished glass samples were recorded on a PerkinElmer (Lambda 950) UV–vis spectrometer in wavelength region of 200–1000 nm. The band position is measured with an accuracy ± 1 nm.

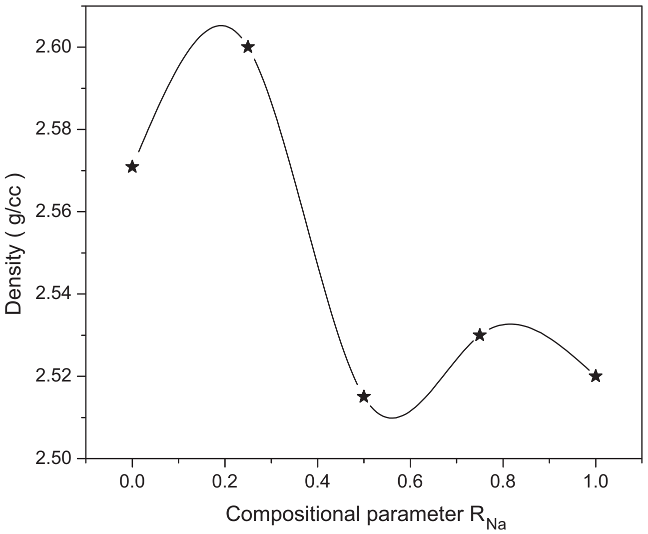

Fig. 1. Density as function of compositional parameter in $(40-x)Li_2O–xNa_2O–10K_2O–50B_2O_3$ glasses.

3. Results and discussion

Fig. 1 presents the room temperature density of mixed alkali $(40-x)Li_2O–xNa_2O–10K_2O–50B_2O_3$ glasses measured by Archimedes method as a function of compositional parameter R_{Na}. From the above figure, it is clear that the density varies non-linearly. The composition-dependent density appears to be ‘waveshaped’, featuring two maxima and one minima. This non-linear behavior is a consequence of mixed alkali effect. The average molecular weight, density, molar volume and oxygen packing density parameters of the present glasses are presented in Table 1. In the present glass system, the molar volume of the glasses increases where as oxygen packing density decreases as the concentration of Na_2O increases, showing no MAE. The oxygen packing density is a measure of the tightness of packing of oxide network. This result indicates that the glass structure becomes loosely packed. Similar observations were found in $Li_2O–K_2O–CdO/ZnO–B_2O_3$ glasses [29].

Modulated differential scanning calorimetry (MDSC) is used to characterize the glass and to determine thermodynamical parameters. The MDSC thermograms of all the glass samples are shown in Fig. 2. The thermodynamical parameters such as glass transition temperature (T_g), crystallization temperature (T_c), glass stability parameter (S) and specific heat capacity difference (ΔC_p), were determined and are given in Table 2. Fig. 3 plots the variation of glass transition temperature as a function of compositional parameter R_{Na}. The glass transition temperature varies non-linearly and exhibited negative deviation indicating the presence of mixed alkali effect in glass transformation temperature. The glass stability S [30] which is defined as the difference between crystallization temperature and glass transition temperature is observed to be less, which may be important for the present glasses as promising material for non-optical applications.

The glass transition temperature of borate glasses is linked with the atomic arrangements present in the glass system. Shelby [31]

Table 1
Composition of the glass system, average molecular weight, density (ρ), molar volume (V_m) and oxygen packing density (OPD).

Glass Composition	Avg. mol. wt. (g/mol)	ρ (g/cc) ± 0.001	V_m (cc/mol)	OPD (g-atm/l)
$40Li_2O–10K_2O–50B_2O_3$	56.81	2.570	21.851	91.528
$30Li_2O–10Na_2O$ $10K_2O–50B_2O_3$	59.3	2.600	22.842	87.558
$20Li_2O–20Na_2O$ $10K_2O–50B_2O_3$	62.6	2.515	22.890	87.374
$10Li_2O–30Na_2O$ $10K_2O–50B_2O_3$	65.8	2.530	26.010	76.890
$40Na_2O$ $10K_2O–50B_2O_3$	69.0	2.520	27.388	73.024

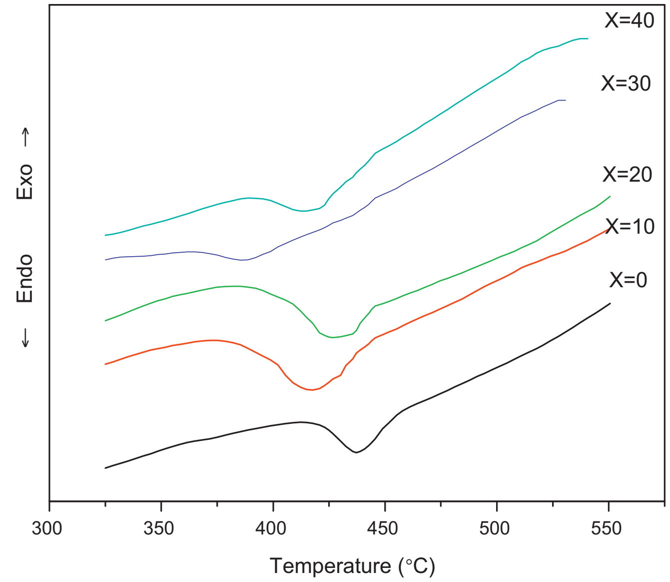

Fig. 2. MDSC thermograms of $(40-x)Li_2O–xNa_2O–10K_2O–50B_2O_3$ glasses.

Table 2
Glass transition temperature (T_g), crystallization temperature (T_c), glass stability (S) and specific heat capacity difference (ΔC_p) of present glasses.

Glass Composition	T_g (°C)	T_c (°C)	S (°C)	ΔC_p (J/mol °C)
$40Li_2O–10K_2O–50B_2O_3$	415	437	22	3.61
$30Li_2O–10Na_2O\ 10K_2O–50B_2O_3$	388	414	26	4.52
$20Li_2O–20Na_2O\ 10K_2O–50B_2O_3$	395	426	31	4.76
$10Li_2O–30Na_2O\ 10K_2O–50B_2O_3$	365	388	23	2.00
$40Na_2O–\ 10K_2O–50B_2O_3$	392	417	25	1.86

Glass stability $S = T_c - T_g$

and Button et al. [32] linked the decrease in T_g with non-bridging oxygens in high alkali region. The negative deviation in glass transition temperature is explained due to the decrease in cross link density, hence decrease in T_g when compared with the end members. The Li^+ and Na^+ ion disturb the structural arrangement of the planar BO_4 units considerably and favors the formation of non-bridging oxygen in glass system. The formation of non-bridging oxygen units cause the depolymerization of the oxide network. The decrease in T_g when compared with end members is attributed to the formation of non-bridging oxygen BO_3 units in present glass system.

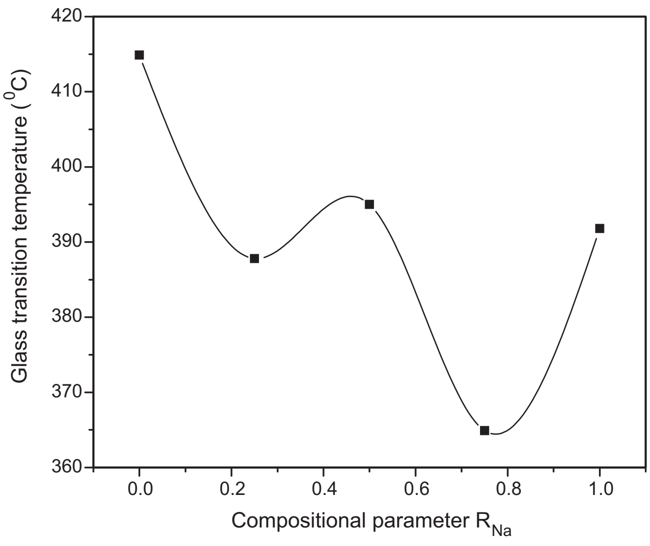

Fig. 3. Glass transition temperature as function of compositional parameter in present glasses.

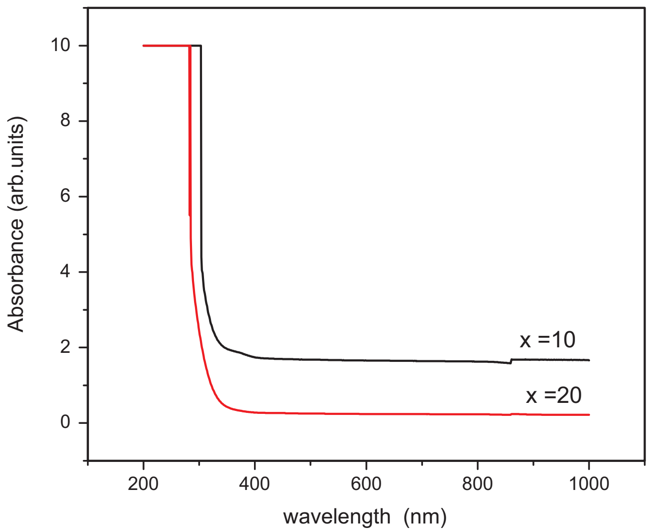

Fig. 4. Optical absorption spectra of $(40–x)Li_2O–xNa_2O–10K_2O–50B_2O_3$ ($x = 10$ and 20 mol%) glasses.

The optical absorption spectra of the present glasses is shown in Fig. 4. Other glass samples in the present series also shows similar spectral behavior. The optical absorption co-efficient $\alpha(\nu)$, near the fundamental absorption edge of the curve in Fig. 4 was determined from the relation

$$\alpha(\nu) = \left(\frac{1}{d}\right) \log\left(\frac{I_0}{I_t}\right)$$

where I_0 and I_t are the intensities of the incident and transmitted beams, respectively, and d is thickness of the glass sample. The factor $\log(I_0/I_t)$ corresponds to absorbance. Davis and Mott [33] and Tauc and Menth [34] relate this data to the optical band gap, E_{opt} through the following general relation proposed for amorphous materials.

$$\alpha(\nu) = \frac{B(h\nu - E_{opt})^n}{h\nu}$$

where B is a constant and $h\nu$ is incident photon energy. The index $n = 1/2$ for direct allowed transitions and $n = 2$ for indirect transition. By plotting $(\alpha h\nu)^{1/2}$ and $(\alpha h\nu)^2$ as a function of photon energy $h\nu$, one can find the optical energy band gap E_{opt} for indirect and direct transitions, respectively. The respective values of E_{opt} are obtained by extrapolating to $(\alpha h\nu)^{1/2} = 0$ for indirect transition and $(\alpha h\nu)^2 = 0$ for direct transition. Fig. 5 represents the Tauc's plots $\{(\alpha h\nu)^{1/2}$ vs $h\nu\}$ for different glass samples. Similar behavior was also observed by other workers [35,36]. The values of the indirect optical energy gap, E_{opt}, thus obtained from the extrapolation of the linear region of Tauc's plots are presented in Table 3. The direct optical energy gap was also determined are presented in Table 3.

Table 3
Optical parameters of $(40-x)Li_2O–xNa_2O–10K_2O–50B_2O_3$ present glasses.

Optical parameters	$x = 0$	$x = 10$	$x = 20$	$x = 30$	$x = 40$
Cut-off wavelength (nm) (±1)	329	349	370	334	356
Indirect optical band gap (eV) (±0.05)	3.76	3.55	3.35	3.71	3.48
Direct optical band gap (eV) (±0.05)	3.77	3.61	3.40	3.72	3.50
Urbach energy ΔE (eV) (±0.01)	0.22	0.19	0.26	0.09	0.11
Electronic polarisabilty $\alpha_{O^{2-}}$ (E_o) (Å^3)	2.36	2.51	2.56	2.80	3.01
Theoretical optical basicity (Λ_{th}) (±0.001)	0.750	0.765	0.78	0.795	0.81
Optical basicity $\Lambda(E_o)$ (±0.001)	0.962	1.005	1.016	1.072	1.115
Interaction parameter $A(E_o)$ (±0.001)	0.080	0.067	0.063	0.047	0.035

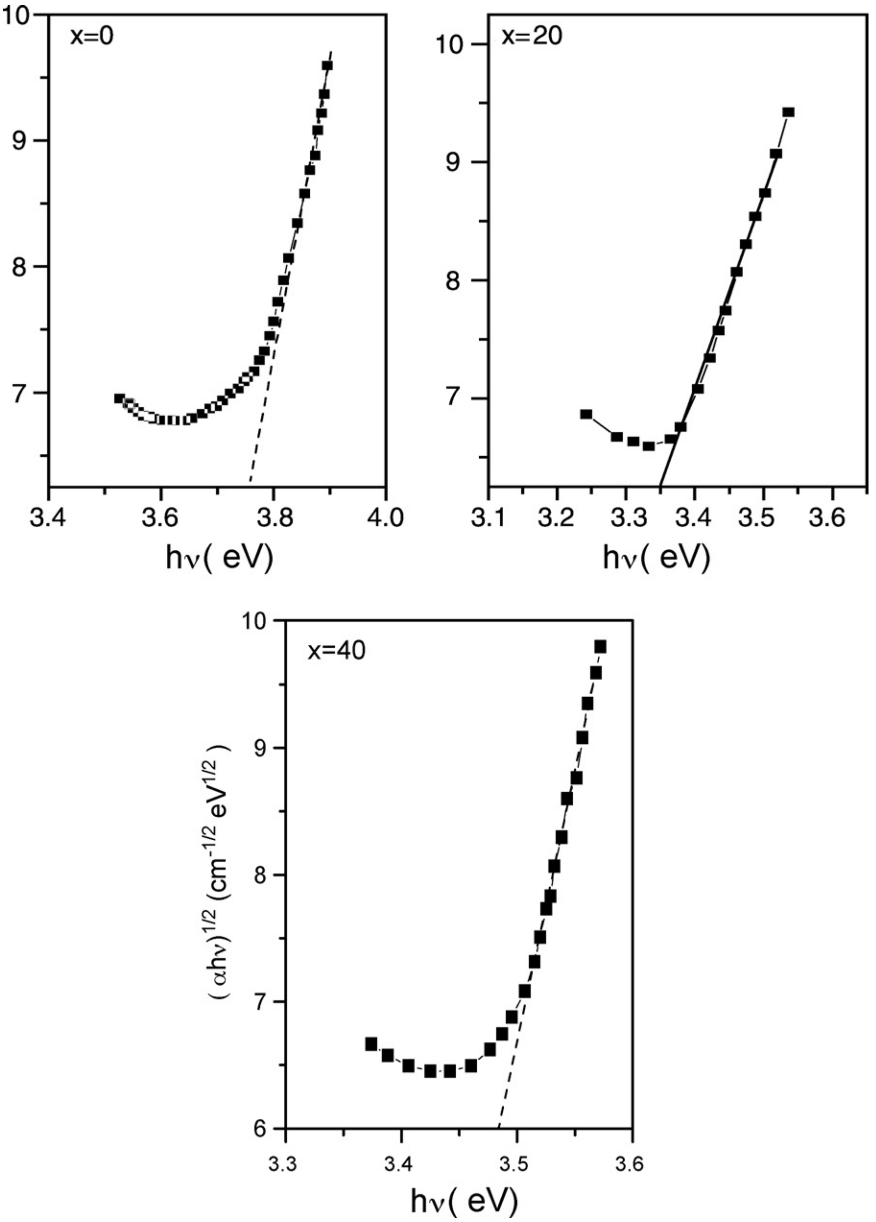

Fig. 5. Tauc's plots for the $(40-x)Li_2O–xNa_2O–10K_2O–50B_2O_3$ ($x = 0$, 20 and 40 mol%) glass system.

The main feature of the absorption edge of amorphous materials is an exponential increase of absorption coefficient $\alpha(\nu)$ with photon energy $h\nu$ and is given by Urbach rule [37]

$$\alpha(\nu) = C \exp\left(\frac{h\nu}{\Delta E}\right)$$

where C is a constant and ΔE is the Urbach energy which is a measure of band tailing. Fig. 6 plots the variation of $\ln(\alpha)$ as function of photon energy $h\nu$. The values of Urbach energy (ΔE) were determined by taking the reciprocals of slopes of the linear portion of $\ln(\alpha)$ vs $h\nu$ curves. The Urbach energy values of the present glass samples are presented in Table 3. The compositional dependence of indirect optical band gap energy, E_{opt}, and Urbach energy ΔE is illustrated in Fig. 7. It is observed that the non-linear variation of band gap energy and Urbach energy with compositional parameter indicates the existence of mixed alkali effect in present glasses.

The electronic polarizability of the oxide ions ($\alpha_{O^{2-}}$) as originally proposed by Dimitrov and Sakka [38] can be calculated on the basis of energy gap data using following equations.

$$\alpha_{O^{2-}}(E_o) = \left[\left(\frac{V_m}{2.52}\right)\left(1-\sqrt{\frac{E_o}{20}}\right) - \sum \alpha_i\right]\left(N_{O^{2-}}\right)^{-1}$$

where V_{m} is the molar volume, $\sum \alpha_i$ denotes molar cation polarizability, $N_{O^{2-}}$ denotes the number of oxide ions in the chemical formula and E_{o} is the optical band gap energy. For a typical glass composition $10Li_2O–30Na_2O–10K_2O–50B_2O_3$, the value of $\sum \alpha_i$ is given by $2[(0.10)\,\alpha_{Li} + (0.30)\,\alpha_{Na} + (0.10)\,\alpha_K + (0.50)\,\alpha_B]$. The values of $\alpha_{Li} = 0.029$ Å^3, $\alpha_{Na} = 0.179$ Å^3, $\alpha_K = 0.083$ Å^3 and $\alpha_B = 0.002$ Å^3 are used. The value of $N_{O^{2-}}$ is equal to 2. The calculated values of $\alpha_{O^{2-}}$ for energy gap data, designated as $\alpha_{O^{2-}}(E_o)$ are presented in Table 3. It is seen that the electronic polarizability increases with increasing sodium content.

An intrinsic relationship proposed by Duffy [39] exists between electronic polarizability of the oxide ions $\alpha_{O^{2-}}$ and optical basicity

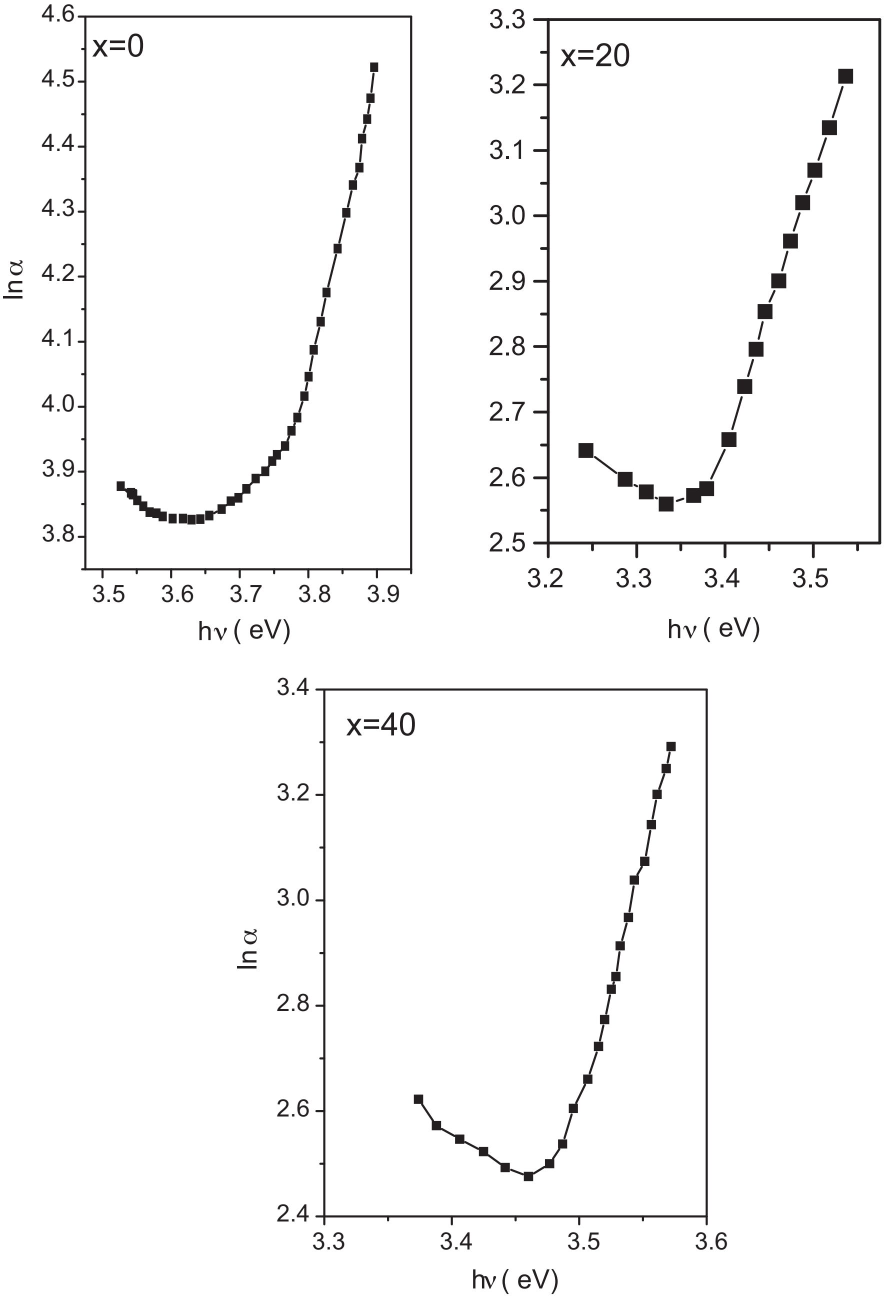

Fig. 6. Plots corresponding ln(α) vs $h\nu$ for $(40-x)Li_2O-xNa_2O-10K_2O-50B_2O_3$ (x = 0, 20 and 40 mol%) glasses.

of the oxide medium Λ and is given by

$$\Lambda = 1.67\left(1-\frac{1}{\alpha_{O^{2-}}}\right)$$

This relation presents a general trend towards an increase in the oxide ion polarizability with increasing optical basicity. The calculated values of optical basicity for energy gap data, designated as $\Lambda(E_o)$ are presented in Table 3. The optical basicity $\Lambda(E_o)$ values increase linearly with increase in sodium content. On the other hand the so-called theoretical optical basicity (Λ_{th}), for the present glasses is calculated using the following equation which is based on the approach proposed by Duffy [39]

$$\Lambda_{th} = x_{Li_2O}\Lambda_{Li_2O} + x_{Na_2O}\Lambda_{Na_2O} + x_{K_2O}\Lambda_{K_2O} + x_{B_2O_3}\Lambda_{B_2O_3}$$

where xLi_2O, xNa_2O, xK_2O and xB_2O_3 are the contents of individual oxides in mol%. Λ_{Li_2O}, Λ_{Na_2O}, Λ_{K_2O} and $\Lambda_{B_2O_3}$ are the theoretical optical basicity values assigned to oxides present in the glass. The values $\Lambda_{Li_2O} = 1$, $\Lambda_{Na_2O} = 1.15$, $\Lambda_{K_2O} = 1.4$, $\Lambda_{B_2O_3} = 0.42$ are used in the present study [38]. The theoretical optical basicity Λ_{th} values calculated using above equation for the mixed alkali borate glasses are presented in Table 3. It is found that the theoretical optical basicity increases slightly with increasing Na_2O content. The variation in glass transition temperature T_g as a function of optical basicity parameter shown in Fig. 8 is non-linear exhibiting the mixed alkali effect.

The interaction parameter is a quantitative measure for the inter ionic interaction of negative ions such as F^- and O^{2-} with the nearest neighbors. Dimitrov and Komatsu [40,41] applied the interaction parameter A proposed by Yamashita and Kurosawa [42] to describe the polarizability state of an average oxide ion in numer-

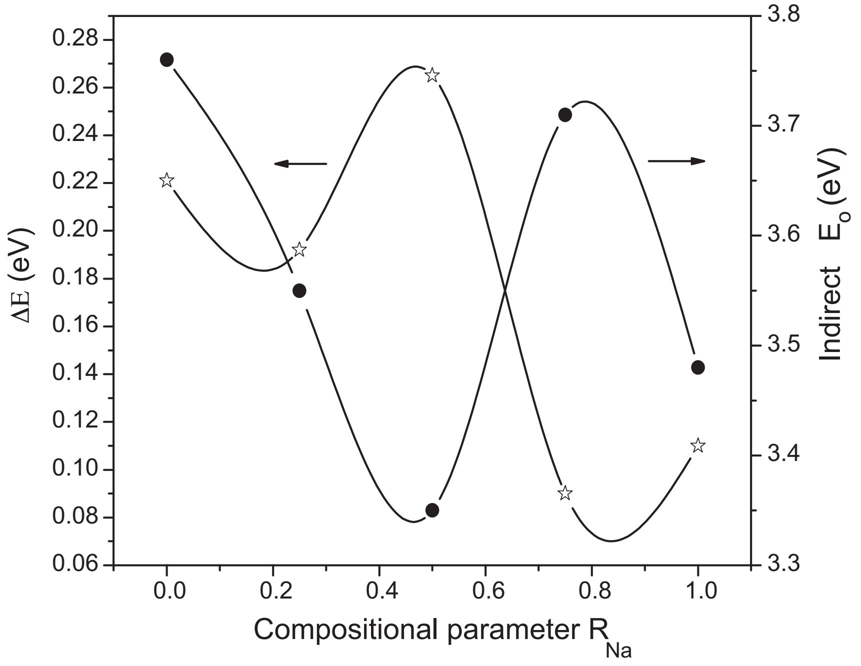

Fig. 7. Compositional dependence of Urbach energy (ΔE) and indirect optical band gap (E_o) in present glasses.

ous simple oxides and its ability to form an ionic covalent bond with the cation. The optical energy based interaction parameter *A(E$_o$)* can be expressed as a sum of the parts each cation with the given oxide ion contributes to the total interaction for an averaged cation anion pair in the glass matrix

$$A = X_{\mathrm{Li_2O}} \frac{\left(\alpha_f^- - \alpha_{\mathrm{O}^{2-}}\right)}{2\left(\alpha_{\mathrm{Li}^+} + \alpha_f^-\right)\left(\alpha_{\mathrm{Li}^+} + \alpha_{\mathrm{O}^{2-}}\right)} + X_{\mathrm{Na_2O}} \frac{\left(\alpha_f^- - \alpha_{\mathrm{O}^{2-}}\right)}{2\left(\alpha_{\mathrm{Na}^+} + \alpha_f^-\right)\left(\alpha_{\mathrm{Na}^+} + \alpha_{\mathrm{O}^{2-}}\right)} + X_{\mathrm{K_2O}} \frac{\left(\alpha_f^- - \alpha_{\mathrm{O}^{2-}}\right)}{2\left(\alpha_{\mathrm{K}^+} + \alpha_f^-\right)\left(\alpha_{\mathrm{K}^+} + \alpha_{\mathrm{O}^{2-}}\right)} + X_{\mathrm{B_2O_3}} \frac{\left(\alpha_f^- - \alpha_{\mathrm{O}^{2-}}\right)}{2\left(\alpha_{\mathrm{B}^{3+}} + \alpha_f^-\right)\left(\alpha_{\mathrm{B}^{3+}} + \alpha_{\mathrm{O}^{2-}}\right)}$$

where α_f^- = 3.921 Å^3, the electronic polarizability of the free oxide ion is used, taking into account the value of ionic refraction of O^{2-} theoretically determined by Pauling [43] and $\alpha_{\mathrm{O}^{2-}}$ corresponds to $\alpha_{\mathrm{O}^{2-}}(E_o)$. The energy gap based interaction parameter $A(E_o)$ determined from the above equation are presented in Table 3.

It has been established that the Yamashita–Kurosawa interaction parameter *A* is closely related to the oxide ion polarizability and

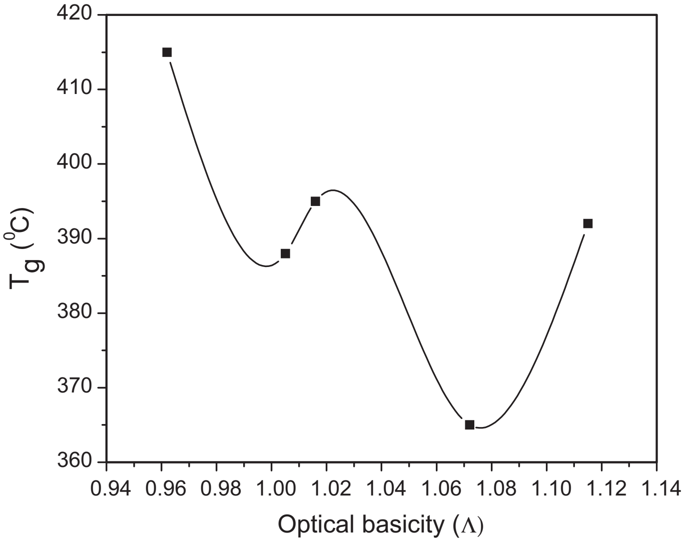

Fig. 8. Variation of T_g as a function of optical basicity in Li$_2$O–Na$_2$O–K$_2$O–B$_2$O$_3$ glasses.

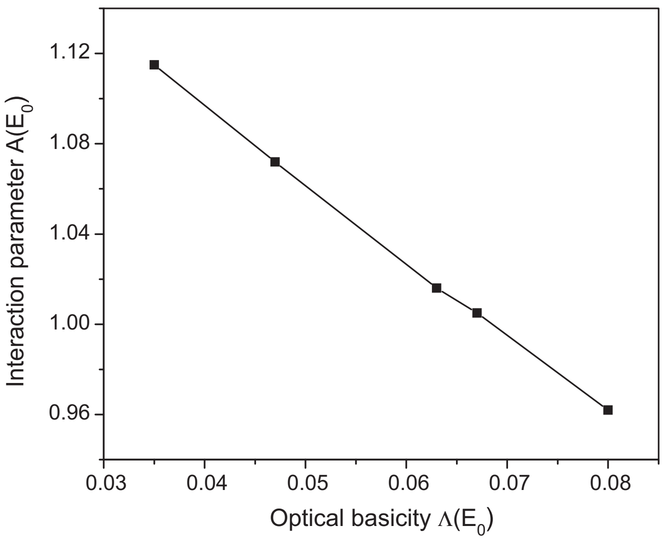

Fig. 9. Relationship between optical basicity $\Lambda(E_o)$ and interaction parameter $A(E_o)$ in the present glasses.

optical basicity of oxide glasses. That is, larger the oxide ion polarizability and optical basicity, the smaller is the interaction parameter. The correlation between interaction parameter A and optical basicity $\Lambda(E_0)$ of the present glasses is shown in Fig. 9, indicating a linear distribution of the optical basicity with respect to the interaction parameter and this can be used as the optical basicity scale for oxide glasses. Based on good correlation among electronic polarizability of oxide ions ($\alpha_{O^{2-}}$), optical basicity (Λ) and interaction parameter (A), the present Li_2O–Na_2O–K_2O–B_2O_3 mixed alkali glasses can be classified as normal ionic (basic) oxides. In general the normal ionic oxides posses intermediate electronic polarizability of oxide ions in the range 2–3 Å^3, optical basicity close to unity and intermediate interaction parameter in the range 0.02–0.08.

4. Conclusions

In this paper, we report, for the first time, the mixed alkali effect in optical studies in borate glasses containing three types of alkali ions. The composition-dependent density appears to be 'wave-shaped', featuring two maxima and one minima. This non-linear behavior is a consequence of mixed alkali effect. The molar volume of the glasses increases where as oxygen packing density decreases as Na_2O content increases, showing no MAE. The glass transition temperature T_g also varies non-linearly, indicating the mixed alkali effect. The indirect optical band gap energy and the Urbach energy in the present glass system varies non-linearly with compositional parameter. Based on good correlation among electronic polarizability of oxide ions, optical basicity and interaction parameter, the present Li_2O–Na_2O–K_2O–B_2O_3 glasses were categorized as normal ionic (basic) oxides. The glass transition temperature varies non-linearly with optical basicity exhibiting the mixed alkali effect.

Acknowledgement

One of the authors (M.A.Samee) wishes to thank the Director, Consortium for Scientific Research, Indore for providing MDSC and optical facilities.

References

[1] D.E. Day, J. Non-Cryst. Solids 21 (1976) 343.
[2] A.H. Dietzel, Phys. Chem. Glasses 24 (1983) 172.
[3] M. Ingram, Glastech. Ber. Sci. Technol. 67 (1994) 151.
[4] B. Roling, M.D. Ingram, J. Non-Cryst. Solids 265 (2000) 113.
[5] G. Domimak-Dzik, W. Ryba-Romanowski, J. Pisarska, W.A. Pisarski, J. Lumin. 122 (2007) 62.
[6] V. Belostotsky, J. Non-Cryst. Solids 353 (2007) 1078.
[7] L. Bih, L. Abbas, S. Mohdachi, A. Nadiri, J. Mol. Struct. 891 (2008) 173.
[8] H.W. Guo, X.F. Wang, Y.X. Gong, D.N. Gao, J. Non-Cryst. Solids 356 (2010) 2109.
[9] M. Seshadri, Y.C. Ratnakaram, D. Thirupathi Naidu, K. Venkata Rao, Opt. Mater. 32 (2010) 535.
[10] P. Maass, A. Bunde, M.D. Ingram, Phys. Rev. Lett. 68 (1992) 3064.
[11] M.D. Ingram, C.T. Imre, I. Konidakis, J. Non-Cryst. Solids 352 (2006) 3200.
[12] A. Faivre, D. Viviani, J. Phalippou, Solid State Ionics 176 (2005) 325.
[13] Y. Gao, Chem. Phys. Lett. 417 (2006) 430.
[14] T. Sankarappa, G.B. Devidas, M. Prashat Kumar, S. Kumar, B.V. Kumar, J. Alloys Compd. 469 (2009) 576.
[15] C.R. Kesavulu, R.S. Muralidhara, J.L. Rao, R.V. Anavekar, R.P.S. Chakradhar, J. Alloys Compd. 486 (2009) 46.
[16] N. Nagaraja, T. Sankarappa, M. Prashanth, Kumar, J. Non-Cryst. Solids 354 (2008) 1503.
[17] A. Vegiri, C.P.E. Varsamis, E.I. Kamitsos, Phys. Rev. B 80 (2009) 184202.
[18] R.P. Sreekanth Chakradhar, B. Yasoda, N. Lakshmana Rao, N.O. Gopal, Mater. Res. Bull. 41 (2006) 1646.
[19] G.N. Hemantha Kumar, J.L. Rao, K. Ravindra Prasad, Y.C. Ratnakaram, J. Alloys Compd. 480 (2009) 203.
[20] C Venkateswarlua, G.N. Hemantha Kumara, M. Seshadria, Y.C. Ratnakarama, K.S.R. Koteswara Rao, J.L. Rao, J. Alloys Compd. 502 (2010) 97.
[21] C.R. Kesavulu, R.P.S. Chakradhar, C.K. Jayasankar, J. Lakshmana Rao, J. Mol. Struct. 975 (2010) 93.
[22] Syed Rahman, R. Shashidhar Bale, Vijaya Kumar, N. Srinivasa Rao, Mat. Res. Bull. 45 (2010) 1533.
[23] N. Srinivasa Rao, M. Purnima, K. Shashidhar Bale, Siva Kumar, Syed Rahman, Bull. Mater. Sci. 29 (2006) 365.
[24] N. Srinivasa Rao, M. Shashidhar Bale, Ch. Purnima, M.A. Srinivasu, K. Samee, Siva Kumar, Syed Rahman, Phys. B: Condens. Matter 404 (2009) 1785.
[25] G. Li, X. Li, W. Luo, Y. Zhang, in: M.K. Choudhary, N.T. Huff, C.N. Drummond III (Eds.), Proceedings of XVIII International Congress on Glass 5–10, July, 1998, The American Ceramic Society, Westerville, OH, 1998.
[26] Y. Gao, C. Cramer, Solid State Ionics 176 (2005) 921.
[27] Y. Gao, C. Cramer, Solid State Ionics 176 (2005) 2279.
[28] M. Kim, W.H. Choi, C.H. Song, G.Y. Jin, Y.H. Rim, Y.S. Yang, Solid State Ionics 180 (2009) 527.
[29] G. Padmaja, P. Kishtaiah, J. Phys. Chem. 113 (2009) 2397.
[30] M. Nalin, M. Poulain, M. Poulain, S.J.L. Ribeiro, Y. Messaddeq, J. Non-Cryst. Solids 284 (2001) 110.
[31] J.E. Shelby, J. Am. Ceram. Soc. 66 (1983) 225.
[32] D.P. Button, R. Tondon, C. King, M.H. Velez, H.L. Tuller, D.R. Uhlmann, J. Non-Cryst. Solids 49 (1982) 129.
[33] E.A. Davis, N.F. Mott, Phil. Mag. 22 (1970) 903.
[34] J. Tauc, A. Menth, J. Non-Cryst. Solids 8 (1972) 569.
[35] A. Agarwal, V.P. Seth, S. Sanghi, P. Gahlot, S. Khasa, Mater Lett. 58 (2004) 694.
[36] R.P. Sreekanth Chakradhar, K.P. Ramesh, J.L. Rao, J. Ramakrishna, J. Phys. Chem. Solids 64 (2003) 641.
[37] F. Urbach, Phys. Rev. 92 (1953) 1324.
[38] V. Dimitrov, S. Sakka, J. Appl. Phys. 79 (1996) 1736.
[39] J.A. Duffy, Phys. Chem. Glasses 30 (1989) 1.
[40] V. Dimitrov, T. Komatsu, J. Ceram. Soc. Jpn. 107 (1999) 1012.
[41] V. Dimitrov, T. Komatsu, J. Ceram. Soc. Jpn. 108 (2000) 330.
[42] J. Yamashita, T. Kurosawa, J. Phys. Soc. Jpn. 10 (1955) 610.
[43] L. Pauling, Proc. R. Soc. London A 114 (1927) 181.